Measurements of the Production and Transport of Helium Ash in the TFTR Tokamak

E. J. Synakowski, R. E. Bell, R. V. Budny, C. E. Bush,* P. C. Efthimion, B. Grek, D. W. Johnson, L. C. Johnson, B. LeBlanc, H. Park, A. T. Ramsey, and G. Taylor

Princeton Plasma Physics Laboratory, Princeton, New Jersey 08543

(Received 24 January 1995)

Helium ash production and transport have been measured in TFTR deuterium-tritium plasmas using charge-exchange recombination spectroscopy. The helium ash confinement time, including recycling effects, is 6–10 times the energy confinement time and is compatible with sustained ignition in a reactor. The ash confinement time is dominated by edge pumping rates rather than core transport. The measured evolution of the local thermal ash density is consistent with modeling based on previously measured helium transport coefficients and classical slowing down of the alpha particles.

PACS numbers: 52.55.Pi, 52.25.Fi, 52.25.Vy, 52.70.Kz

Helium ash production, transport, and removal will play a decisive role in determining the cost and the viability of a deuterium-tritium fusion reactor based on magnetic confinement schemes. Studies [1–5] indicate that ash concentration, and ultimately its reduction, in a future reactor will depend critically on the relationship between energy transport and helium particle transport in the plasma core, as well as particle reflux properties at the plasma boundary. If transport of helium ash from the core to the edge is slow compared to its production rate, the ash may quench the burn before any significant pumping can take place. Moreover, even if the core helium transport is rapid, inefficient edge pumping or reduced edge transport might lead to intolerably high central ash densities.

Deuterium-tritium (DT) operation on TFTR [6,7] provides the first opportunity to observe the production of helium ash and its transport. Although the fusion power in these plasmas (~5 MW) is modest by reactor standards, the on-axis helium ash source strength is comparable to that expected for ITER. Also, while a reactor-relevant helium pumping scheme needs to be developed, the TFTR bumper limiter pumps helium and other noble gases [8]. These facts enable the study of a prototypical reactor with all the essential elements as they pertain to ash birth, transport, and removal. As such, DT operation allows testing of expectations from earlier helium transport experiments [9–13] that have generally concluded that core helium transport should be fast enough to remove helium ash from the plasma center, before significant accumulation can occur, and deposit it in the plasma periphery, where it might be pumped.

Presented in this Letter are the first measurements of the transport of helium ash born in a deuterium-tritium tokamak plasma. Pairs of similar deuterium-only (DD) and DT plasmas were investigated. The measurements were made using charge-exchange recombination spectroscopy (CHERS) [14]. The thermal helium density n_{He} was inferred by observing Doppler-broadened emission from the 4686 Å, n = 4-3 He^{+} line, excited by charge exchange between deuterium heating beam neutrals and He^{2+}. These measurements present a particular challenge. Carbon lines, excited by electron impact and charge exchange, are present at or near 4686 Å. Although weak by most standards, they provide a comparatively bright background for the emissions from helium ash, whose concentration is expected to be only (0.1–0.2)% of the electron density.

An array of fiber optics was used which views three of the heating beam sources on the plasma midplane. The sightlines cross the beams with a radial separation of 6 cm and span the plasma outside the magnetic axis. The integration time of the CHERS diagnostic was 0.1 s. The plasmas had a major radius of 2.52 m, a minor radius of 0.87 m, and a plasma current of 2.0 MA. For the DD and DT cases, approximately 21–22 MW of nearly balanced neutral beam power was injected from 2.8 to 4.1 s into a deuterium target plasma. For both plasmas, deuterium-only injection at lower power (12 MW) followed this phase, ending at 4.8 s. The fusion power during the neutron flattop was about 4.5 MW. The central ion temperature $T_i(0)$, measured viewing the 5292 Å charge exchange line (n = 8-7) of C^{5+}, reached 25 keV, dropping to 18 keV during the 12 MW injection period. The central electron temperature $T_e(0)$, measured with a Michelson interferometer, was 9 keV in the high power period of both plasmas, and dropped to 7 keV in the latter phase. The central electron density was $(6.7–7) \times 10^{19} \mathrm{m}^{-3}$ in the high power phase of each discharge, falling to $4.5 \times 10^{19}\ \mathrm{m}^{-3}$ in the 12 MW portion. The central Z_{eff}, inferred from visible bremsstrahlung (VB) measurements, was 3 during high power injection, dropping to 2.4 in the 12 MW period. The enhancement factor over L mode energy confinement time values was 1.9 during high-power injection, and 1.4 in the latter phase. Sawteeth did not occur in the DT discharge until 4.78 s, 20 ms prior to the end of neutral beam injection, and were absent from the DD discharge. Fiber transmission dropped transiently by 9% during tritium injection due to high neutron and gamma fluxes [15]. Its time dependence was measured directly with a calibration loop [16], and the effect was taken into account in this experiment.

0031-9007/95/75(20)/3689(4)$06.00

Modeling indicates that the slowing-down time of the alpha particles should be 0.5–0.7 s, and that alpha particles should continue to thermalize in the core throughout the deuterium-only heating period. The measured neutron emission and the calculated volume-integrated thermal helium source due to the slowing-down of confined alpha particles are shown in Fig. 1 for the DT plasma. The ash source was calculated with the TRANSP code [17], using measured plasma profiles, calculated beam deposition, and calculations of the alpha particle source and transport. The alpha particles are assumed to transport classically until their energy is equal to $\frac{3}{2}$ the local ion temperature. Alphas that fall below this energy are declared to be helium ash particles and are subject to prescribed transport coefficients. The measured [18,19] and modeled neutron emissivity profiles are similar in shape and amplitude. Both are strongly peaked, and have a half width at half maximum of about 20% of the minor radius of the plasma. Modeling indicates that the energetic alpha particle transport should be modest, and that the helium ash thermalization profile should have the same shape as that of the neutrons. Measurements of the confined energetic alpha energy distribution [20,21] are consistent with good confinement and classical transport of the alpha particles. Also, probe measurements indicate that the alpha particle losses are small [22]. Measured values of the helium diffusivity D_{He} and the convective velocity V_{He}, inferred from a 1 MA plasma [11], were used in the modeling. The 1 MA plasma had particle and energy confinement times similar to the 12 MW phase of the plasmas examined here. The thermal conductivity χ_{eff} for the these two plasmas were similar as well. Since past observations indicate that D_{He} is correlated with χ_{eff} in different confinement regimes on TFTR [11], this choice of transport coefficients is reasonable. For $r/a > 0.5$, D_{He} is

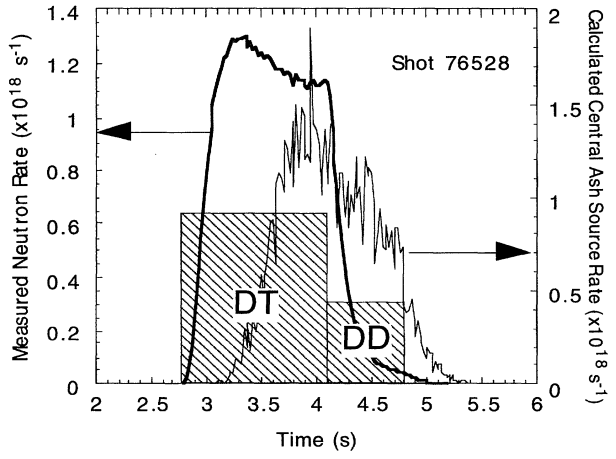

FIG. 1. The measured total neutron rate and the calculated rate at which alpha particles are joining the population of thermal particles in the DT plasma. The shaded regions indicate the relative powers and durations of the two neutral beam heating phases.

1–2 $\mathrm{m^2\,s^{-1}}$, falling to about 0.4 $\mathrm{m^2\,s^{-1}}$ near $r/a = 0.2$. The convective pinch V_{He} is inward and on the order of -1 m/s near the axis, near zero at $r/a = 0.5$, and ~ -5 m/s near the plasma periphery.

The ash density profile is inferred from the difference in the total beam-induced line brightnesses measured in the DT and DD shot. The expected spectrally integrated ash signal is at least 10 times larger than the photon and readout noise [23] on the total signal, indicating that plasma-to-plasma variations, and not photon statistics, determine the feasibility of detecting ash in these plasmas. Extracting the ash brightness from the other components in the same wavelength interval cannot be performed by standard fitting techniques with Gaussian line shapes: Multiple solutions are possible, and plume emission [24] results in potentially non-Gaussian line profiles. However, the technique used here does not require detailed line fitting of the various components of the spectrum. At the end of the neutral beam phase, the total brightness of the edge emission, measured just after beam turn-off, was subtracted from the total brightness measured just prior to beam turn-off. A correction of about 10% in the edge brightness, resulting from the decay of the emission following beam turn-off, was applied, and was determined by observing the edge emission behavior with high time resolution (10 ms) in similar plasmas. The time behavior of the beam-induced line brightness was extracted by modeling the time behavior of the brightness of the edge emission [25] and subtracting it from the measured total brightness.

To obtain the ash density profile, a trial helium density profile is input into a beam attenuation and plume correction code that calculates the beam deposition, charge exchange emissivity, and parallel transport and emission of plume ions. From the calculated toroidal and radial velocity distribution of the He^+ charge exchange products, the total helium ash line brightness is calculated for each sightline. The measured and modeled beam-induced brightness profiles are compared, and the trial helium ash profile is iterated until agreement between the measured and calculated brightness profiles is achieved. Plasma profiles, including $T_i(R)$ and the toroidal rotation velocity $V_\phi(R)$ inferred from 5292 Å carbon emission from a similar plasma, were used in the calculations.

At 3.45 s, before alpha particles are expected to be thermalized, the spectra from the DD and DT plasmas for a given sightline passing through the core are indistinguishable, highlighting the similarity of these discharges [Fig. 2(a)]. The emission is from the dominant impurity of TFTR, carbon. The dominance of carbon in the absence of helium ash in these spectra was confirmed in two ways. First, using recent calculations of the charge exchange emission cross sections [26], the brightness of the charge exchange component [C^{5+}, 4686 Å, n = 12-9; Fig. 2(b)] yields carbon densities that are consistent with Z_{eff} values inferred from VB measurements. Also, the T_i profile measured with this line agrees with that obtained from similar plasmas with the 5292 Å C^{5+} line.

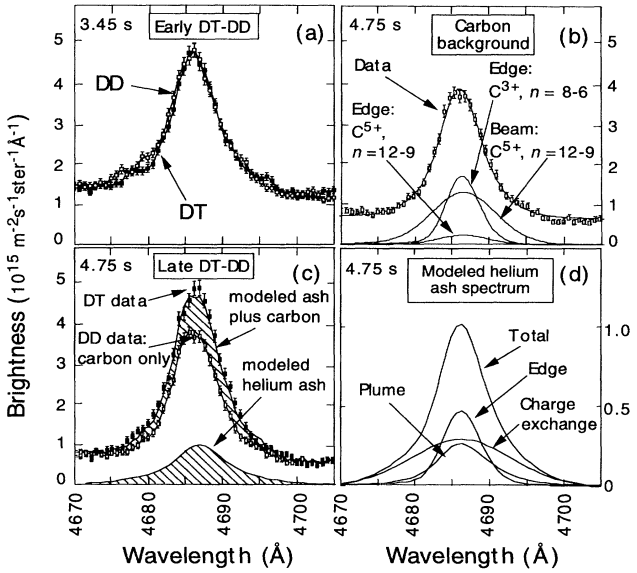

FIG. 2. Spectra from a sightline passing through the neutral beam at $r/a = 0.38$. Instrumental broadening is about 4 Å. (a) Spectrum for the DT-DD plasma pair at 3.45 s, during the high-power phase of injection, and before the expected arrival of helium ash. (b) Spectrum for the DD case at the end of the 12 MW phase of injection. (c) Measured spectra for the DD and DT plasmas late in time (4.75 s). Also shown is the sum of the DD spectrum and the simulated ash spectrum. (d) Simulated ash spectrum for 4.75 s.

In Fig. 2(b), the total edge brightness was inferred from the measured decay after beam turn-off. Emission from C^{3+} ($8h$-$6g$, $8g$-$6h$, and $8i$-$6h$; near 4686 Å) dominates the edge portion of this spectrum. This was verified by comparing measured and calculated [27,28] emission ratios between these three lines and the C^{3+} $6h$-$5g$ line (4658 Å). The relative brightnesses of the core (charge exchange) and edge (electron impact) $n = 12$-9 lines, as well as this edge line's width, were determined from measurements of corresponding components of the 5292 Å line, and the ratios of the cross sections for each process and transition.

Late in time, a distinct increase in the brightness of the thermal portion of the CHERS spectrum is found in the DT plasmas as compared to their DD counterparts, corresponding to a local increase in the helium density in DT as compared to DD [Fig. 2(c)]. This enhancement in DT is seen on all spatial channels, and in other DT-DD shot pairs. This increase is not due to a change in carbon density. From measurements of the 5292 Å line in other similar pairs, the carbon density is the same at any given time to within a few percent. Also, an increase in the carbon density that would lead to this change in brightness would appear as an increase in the measured Z_{eff} of about 0.3 in DT as compared to DD; this is not observed. The local ash density corresponding to the beam-induced brightness is about 3.5×10^{16} m^{-3}, consistent with TRANSP predictions (see below). By using the calculated radial and toroidal He^+ velocity distributions, the spectrum of the plume and prompt ash emission has been simulated [Fig. 2(d)]. The sum of this ash spectrum with the carbon emission from the D-D plasma is in good agreement with the spectrum of the D-T plasma [Fig. 2(c)]. The ratio of the brightnesses of the edge and beam-induced components was determined by helium gas puffing into similar plasmas.

The radial helium ash profile shape and total particle number late in time indicate that the ash transports rapidly from the central source region to the plasma periphery, where it is pumped. Measured and modeled profiles are shown in Fig. 3(a) for 4.75 s. The measured profile shape is broad, in agreement with the modeling. The measured total ash particle number agrees with the TRANSP simulations only if the recycling coefficient R_{He} is below unity. A value of 0.85 was used since it reproduces helium decay times following a short gas puff in plasmas with similar working gas wall pumping characteristics. Under the assumption of zero radial transport (perfect confinement), the modeled profile shape is much more peaked than that measure, and yields a total helium particle number that is larger by a factor of 2. If the central source were turned off, the profile scale length is predicted to relax to that given by the bottom of the shaded region in Fig. 3(a). This illustrates the dominance of the transport over the central source in determining the profile shape.

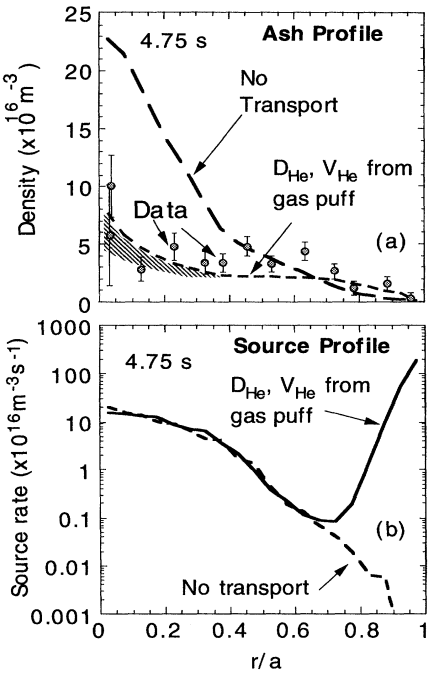

FIG. 3. (a) Measured and modeled ash profile shapes just prior to the end of beam injection. The errors include uncertainties in the plume correction, beam attenuation, background emission subtraction, charge exchange emission rates, photon statistics, and reproducibility of background carbon levels. The shaded region represents the difference in the profile shapes that are predicted with and without the central source, but with transport in both cases. (b) Modeled total helium ash source profiles.

The total helium ash residence time in the vacuum vessel, τ^*_{He}, is 1.2 ± 0.4 s, about $(6-10)\tau_E$, and is consistent with the requirements for a sustained fusion burn in a reactor [3]. Here, τ_E is the global energy confinement time. The residence time was determined from the continuity equation, $dN_{He}/dt = -N_{He}/\tau^*_{He} + S_{He}$, where N_{He} is the measured total helium ash particle number and S_{He} is the calculated volume-integrated alpha particle thermalization (central ash source) rate. This value of τ^*_{He} agrees with that deduced independently from helium gas puffing. However, the helium particle confinement time τ_{He} (which does not include recycling effects), obtained with the calculated central ash source profile and the measured D_{He} and V_{He}, is about 0.3 s, or $2\tau_E$. Therefore, edge reflux, and not core transport, will be the limiting factor determining helium removal from a reactor-grade plasma with core transport mechanisms similar to TFTR supershots. The dominance of the edge source over the central source late in time is illustrated in Fig. 3(b).

The modeled helium ash time evolution indicates that the alpha particle slowing-down calculations and transport assumptions are consistent with measurements. Best agreement between the modeling and the measurement is obtained using the measured values of D_{He} and V_{He} [Figs. 4(a) and 4(c)]. Also, assuming the transport model is valid, the time histories are consistent with the alpha slowing-down time being governed by classical collisional processes. When the slowing-down rate is varied by a factor of 2, the data fall within the predicted range of time histories [Figs. 4(a) and 4(b)]. The time behavior is inconsistent with large-scale anomalous energetic alpha particle losses. Burial of promptly lost alphas would result in a discrepancy between observed and predicted ash densities, while reflux of lost energetic alphas as thermal helium would result in the appearance of ash earlier than observed.

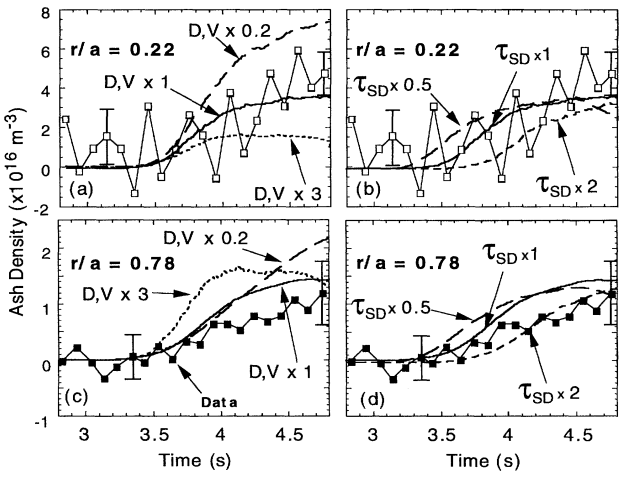

FIG. 4. The measures helium ash density evolution, and modeling results based on TRANSP simulations of the alpha particle slowing down and subsequent transport and wall pumping of the thermalized ash. (a) Data and simulations for $r/a = 0.22$. The simulations were obtained using multiplying factors of 0.2, 1.0, and 3.0 on the nominal values of $D_{He}(r)$ and $V_{He}(r)$, described in the text. (b) Same as (a), but with simulations obtained by varying the alpha particle slowing down time τ_{SD} by factors of 0.5 and 2, using the nominal transport coefficients. (c) Same as (a), but for $r/a = 0.78$. (d) Same as (b), but for $r/a = 0.78$.

It is a pleasure to acknowledge the support of the TFTR physicists, engineers, technical staff, and computer operators. R. E. Olson (University of Missouri) and R. E. H. Clark (Los Alamos) are gratefully acknowledged for their generous responses to requests for atomic physics calculations. This research was conducted under DOE Grant No. DE-AC02-76-CHO-3073.

*Permanent address: Oak Ridge National Laboratory, Oak Ridge, Tennessee 37830.

[1] F. Engelmann, Comments Plamsa Phys. Controlled Fusion **5**, 261 (1980).
[2] R. J. Taylor, B. D. Fried, and G. J. Marales, Comments Plasma Phys. Controlled Fusion **13**, 227 (1990).
[3] D. Reiter, G. H. Wolf, and H. Kever, Nucl. Fusion **30**, 2141 (1990).
[4] M. H. Redi and S. A. Cohen, Fusion Technol. **20**, 48 (1991).
[5] M. H. Redi, S. A. Cohen, and E. J. Synakowski, Nucl. Fusion **31**, 1689 (1991).
[6] R. J. Hawryluk *et al.*, Phys. Rev. Lett. **72**, 3530 (1994).
[7] J. D. Strachan *et al.*, Phys. Rev. Lett. **72**, 3526 (1994).
[8] A. T. Ramsay and D. M. Manos, J. Nucl. Mater. **196–198**, 509 (1992).
[9] E. J. Synakowski *et al.*, Phys. Rev. Lett. **65**, 2255 (1990).
[10] D. L. Hillis *et al.*, Phys. Rev. Lett. **65**, 2382 (1990).
[11] E. J. Synakowski *et al.*, Phys. Fluids B **5**, 2215 (1993).
[12] M. R. Wade *et al.*, General Atomics Report No. GA-A21702, 1994.
[13] H. Nakamura *et al.*, Phys. Rev. Lett. **67**, 2658 (1991).
[14] B. C. Stratton *et al.*, in *Proceedings of the IAEA Technical Committee Meeting on Time Resolved Two- and Three-Dimensional Plasma Diagnostics, Nagoya, Japan* (International Atomic Energy Agency, Vienna, 1991), p. 78.
[15] A. T. Ramsey, Rev. Sci. Instrum. **66**, 871 (1995).
[16] C. E. Bush, R. E. Bell, and E. J. Synakowski, Rev. Sci. Instrum. **66**, 642 (1995).
[17] R. Budny *et al.*, Nucl. Fusion **32**, 429 (1992).
[18] L. C. Johnson, Rev. Sci. Instrum. **63**, 4517 (1992).
[19] A. L. Roquemore *et al.*, Rev. Sci. Instrum. **61**, 3163 (1990).
[20] G. McKee *et al.*, Phys. Rev. Lett. **75**, 649 (1995).
[21] R. Fisher *et al.*, Phys. Rev. Lett. **75**, 846 (1995).
[22] S. J. Zweben (to be published).
[23] R. E. Bell *et al.*, Rev. Sci. Instrum. **63**, 4744 (1992).
[24] R. J. Fonck, D. S. Darrow, and K. P. Jaehnig, Phys. Rev. A **29**, 3288 (1984).
[25] E. J. Synakowski, R. E. Bell, and C. E. Bush, Rev. Sci. Instrum. **66**, 649 (1995).
[26] R. E. Olson (private communication).
[27] R. E. H. Clark (private communication).
[28] J. Abdallah *et al.*, J. Quant. Spectrosc. Radiat. Transfer **50**, 91 (1993).